Theoretical and Applied Climatology (2021) 145:1145–1159
https://doi.org/10.1007/s00704-021-03687-w

ORIGINAL PAPER

Prediction and correction of in situ summer precipitation in Southwest China based on a downscaling method with the BCC_CSM

Qu Guo[1] · Xiangwen Liu[2] · Hongyu Tang[1] · Yonghua Li[1]

Received: 21 January 2021 / Accepted: 4 June 2021 / Published online: 18 June 2021

Abstract

To predict summer precipitation in Chongqing in Southwest China, a downscaling method targeted at the interannual increment of predictand instead of the interannual anomaly of predictand is developed with the Beijing Climate Center Climate System Model (BCC_CSM). Predictions of precipitation, geopotential height, winds, and sea surface temperature by the BCC_CSM and the precipitation observations from 34 weather stations in Chongqing in Southwest China during 1991–2018 are used to establish and validate the method. Specifically, for each of the 34 stations, correlations between the interannual increment of precipitation at the station and the above predicted variable fields in the globe are examined, and the key regions with the highest correlation coefficients are then selected. The predicted variables over these regions are treated as the optimal predictors and are further used to establish three kinds of regression functions for predicting the interannual increment of precipitation. Finally, summer precipitation is predicted by adding the forecasted interannual increment in the target summer onto the observation in the previous summer. Results show that the original precipitation predicted by the BCC_CSM is obviously underestimated in Chongqing. The downscaling predictions, especially the one based on the multivariate stepwise regression approach, achieve reasonable prediction accuracy across years and sites. For the forecasts starting at March 1st, April 1st, May 1st, and June 1st, the skill scores for summer precipitation prediction increase from 80.7, 41.9, 82.8, and 43.5 to 82.5, 66.7, 86.2, and 86.6 in 2017, and from 89.8, 82.8, 55.3, and 85.8 to 91.4, 83.7, 78.1, and 93.2 in 2018, respectively. In addition, the downscaling method could better predict the abnormal-rainfall areas in Chongqing.

1 Introduction

Reasonable predictions of seasonal-scale climate variables are urgently needed for meteorological forecasting, which faces many difficulties and challenges. Dynamic prediction using numerical climate models developed rapidly over the past 20 years. It is one of the main effective methods for seasonal climate forecasts. Many countries have established seasonal climate forecast models and achieved continuous improvement in model forecasting. It was indicated that performance of climate (especially summer precipitation) prediction by the pure dynamic prediction models was usually limited (Gong et al. 2018). The finite resolution, uncertain initial conditions, and imperfect physical processes included in dynamic models generate inevitable errors in climate predictions (Bollasina and Ming 2013; Jiang et al. 2016). To correct the prediction skills, the strategy was developed by combining statistics with predictions from dynamic models (Fan and Wang 2009; Hu et al. 2013; Li and Wang 2018; Wang et al. 2018). However, there were still great uncertainties in short-term climate predictions due to many complex factors (Wang et al. 2016). Thus, improvement of climate models and prediction methods would be a long-term requirement for meteorological departments worldwide.

The Beijing Climate Center Climate System Model Version 1.1 with a moderate resolution (BCC_CSM1.1(m)) was developed by the Beijing Climate Center (BCC) in 2015. This model has been used in the seasonal climate prediction operation. The BCC_CSM1.1(m) shows reasonable performances in simulating and predicting the summer climate mean state and variability (Kan et al. 2015; Liu et al. 2014). Particularly, the variability of the seasonal-to-interannual summer circulation in the Asia–Pacific region could be

✉ Qu Guo
guoqu510@163.com

✉ Xiangwen Liu
xwliu@cma.gov.cn

[1] Chongqing Climate Center, Chongqing Meteorological Administration, Chongqing 401147, China

[2] National Climate Center, China Meteorological Administration, Beijing 100081, China

skillfully predicted, especially for the Southeast Asian summer monsoon (Liu et al. 2015). It was also found that the predicted large-scale circulation variables (e.g., atmospheric circulation and sea temperature) usually carry good related information for site-specific precipitation predictions (Kang et al. 2011).

However, due to the uncertainty and complex interactions among various factors, it was difficult to predict short-term climate variables. Also, inconsistent signals between the interannual and interdecadal variability increase the difficulty of the predictions. Fan et al. (2008 2009) used the interannual increment method to correct the prediction of precipitation and circulation. It focused on prediction of interannual increment relative to the previous year rather than prediction of interannual anomaly in the forecast year. Fan and Wang (2009) reported that the interannual increment could accurately reflect the quasi-biennial variation characteristics of climate variables and sensitively reflect the dynamic changes in the climate variables, amplify abnormal signals, and significantly reduce the influence of the interdecadal background.

Another effective way to improve short-term prediction ability is combining model outputs with statistical downscaling methods (Juneng et al. 2010; Fan et al. 2012; Liu and Fan 2014). Wang et al. (2020) used the stepwise pattern projection method to improve the prediction of the two types of ENSO. Zhu et al. (2008) used the empirical orthogonal function (EOF) and singular value decomposition (SVD) methods to predict the summer monsoon precipitation anomaly and improve the precipitation prediction in the South China Sea. Besides, selecting the circulation variables with high prediction skill and physical connection as the predictors to establish the prediction model can achieve better predictions (Paul et al. 2008). In addition, Gu et al. (2011) searched the areas that were closely related to the regional precipitation, used the model predictions at the grids within the high-skill area as predictor, and further established downscaling forecast scheme and improved the prediction accuracy of regional precipitation.

Located in the eastern Qinghai-Tibet Plateau, Chongqing area in Southwest China has a complex and diverse geological structure, including basins, hills, and other topographical features. The unique geographic and climate characteristics result in complex change of atmospheric motion and high probabilities of flooding and various kinds of geological disasters. Therefore, there is both scientific and practical significance to explore the influencing factors of summer precipitation anomalies over the above area and further establish a reliable forecast method. In this study, we establish a downscaling method to correct the prediction of summer precipitation in Chongqing area in Southwest China based on the BCC_CSM1.1(m). The main objectives are to (1) evaluate the accuracy of original summer precipitation prediction of the BCC_CSM1.1(m) in Chongqing area and (2) evaluate the validity of downscaling method in correcting the precipitation predictions of the BCC_CSM1.1(m). This study is expected to provide a new strategy for seasonal prediction of in situ summer precipitation in Southwest China.

2 Model, data, and methods

2.1 Model

The BCC_CSM1.1(m) for seasonal climate prediction operation at the BCC is used in this study. This model is a medium-resolution global climate system model incorporating atmospheric, oceanic, land surface, and sea ice processes. It is one of the climate system models being used in the Coupled Model International Comparison Program phase five (CMIP5). The atmospheric component mode adopts BCC_AGCM2.2 with a T106 horizontal resolution (equivalent to 1.125°×1.125°) and 26 hybrid sigma/pressure layers in the vertical direction (Wu et al. 2010). The land surface component of the model is BCC_AVIM1.0, which was established based on the common land surface model physical module of a dynamic vegetation and soil carbon cycle model developed by the National Center for Atmospheric Research (NCAR) (Ji et al. 2008). The ocean component of the model adopts the Geophysical Fluid Dynamics Laboratory Modular Ocean Model version 4 (MOM4; Murray 1996) and the Sea Ice Simulator (SIS; Winton 2000). The horizontal resolution of MOM4 was 1° in the mid-high latitudes and 1/3° in the tropics, and the model includes 40 layers in the vertical direction. Each component mode was directly and dynamically coupled with a coupler (CPL5.0). More details about the dynamic frameworks and the main physical processes of BCC_CSM1.1(m) could be found in Wu et al. (2013).

Focusing on the prediction of climate in summer (June–August), hindcast experiments by the BCC_CSM1.1(m) were carried out on March 1, April 1, May 1, and June 1 in each year with lead times of 3 months (LM3), 2 months (LM2), 1 month (LM1), and 0 months (LM0), respectively. Atmospheric initial conditions were obtained from the four times daily temperature, winds, and surface pressure reanalysis products published by the National Center for Environmental Forecasting (NCEP). The ocean initial conditions were obtained from the ocean temperature reanalysis by the NCEP Global Ocean Data Assimilation System. The ensemble prediction strategy adopted the lagged average forecasting (LAF) method, and each hindcast contains 15 members, which were generated based on the combination of the initial atmospheric values in 5 days before the prediction and the initial ocean values in 3 days before the prediction.

2.2 Data

Two datasets are used in this study: (1) daily observed precipitation from the 34 weather stations in Chongqing during 1991–2018. The geographical distribution of stations is given in Fig. 1; (2) the precipitation, 500-hPa geopotential height (H_{500}), 850-hPa zonal wind (U_{850}), 850-hPa meridional wind (V_{850}), and SST fields from the hindcast experiments of BCC_CSM1.1(m) during 1991–2018. The bilinear interpolation method is used to interpolate the hindcast data from model grids to stations.

2.3 Method

2.3.1 Downscaling prediction of precipitation

In this study, the predicted H_{500}, U_{850}, V_{850}, and SST are used as predictors for prediction of precipitation at each station. The large-scale circulation variables are usually treated as good predictors with useful information for precipitation prediction (Kang et al. 2009; 2011). In addition to the good statistical relationship between precipitation

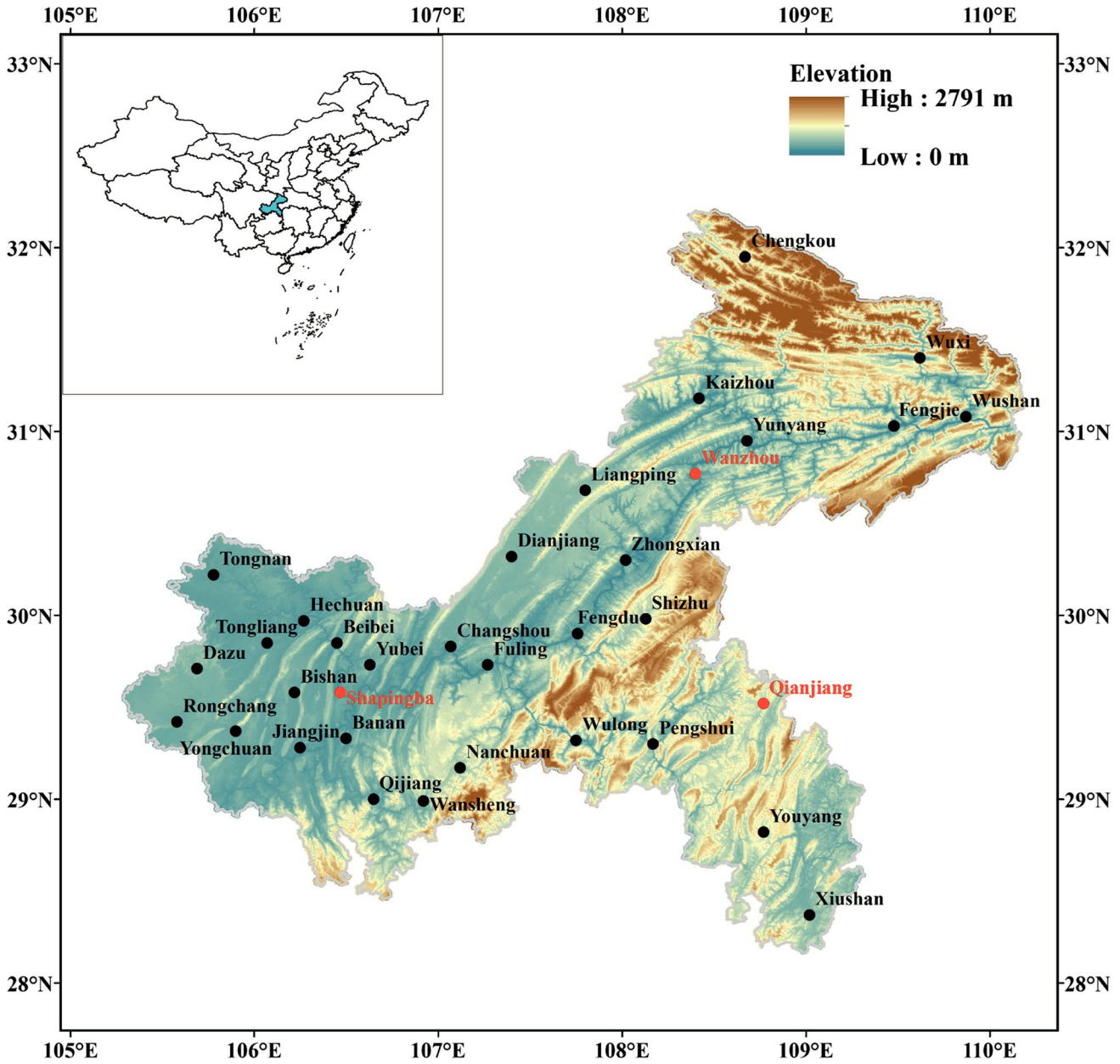

Fig. 1 Locations of the 34 weather stations in Chongqing, southwest China. Red dots show the three typical stations in northeast (Wanzhou), southeast (Qianjiang), and southwest (Shapingba) Chongqing, respectively

and predictors of circulation, there were sometime reliable connections in physical mechanisms.

Then, relationships among the interannual increment of the above four predictors and the interannual increment of observed precipitation at each station are examined. To avoid the interference of small-scale information, the global field of each predictor is divided into many spatial windows with $10° \times 10°$ grid range. For each window, the correlation coefficient between the interannual increment of each predictor averaged over the spatial window and the interannual increment of observed precipitation at the target station is calculated. A global scanning of the windows is done and the window with the highest absolute correlation coefficient is selected as the optimal window. To improve the correlation, in the optimal window, the grids with absolute correlation coefficient greater than the correlation coefficient of the whole window are selected. Since the grids in each window are distributed with close distance, the correlation coefficients over these grids have the same sign (positive or negative). Finally, the predictor averaged over the selected grids is treated as the optimal predictor for the prediction of precipitation at the target station.

Further, regression functions of predictand to predictor are established and validated for the prediction of interannual increment of summer precipitation. Regression analysis has been widely used to analyze the relationship between predictand and predictors. According to the optimal predictors selected in the above step, the single-factor linear regression, the stepwise multiple regression (S-Reg), and the multiple regression (M-Reg) functions are built for predicting the interannual increment of precipitation at the 34 weather stations. In this study, the observation and hindcast data from 1991 to 2013 is used to establish the regression functions, while the data from 2014 to 2018 is used to validate these regression functions. Kug et al. (2008) pointed out that data length shorter than 30 years may be not enough to establish a stable statistical relationship, and the reliability of relationship would degrade significantly if the length of data decreases further. Since the data length in our study is less than 30 years, cross-validation (CV) is employed to test the reliability and accuracy of the downscaling method. CV is a method that statistically slices a sample into smaller subsets (Kohavi 1995), which can be usually divided into *k*-fold CV and leave-one-out CV (LOO-CV). LOO-CV is employed to test the reliability of precipitation prediction in this study. Specifically, each of the 23 years is treated as the testing year, and the rest years are used for training the regression functions and establishing an approach for prediction of precipitation in the testing year. Finally, using the above downscaling method, in situ precipitation prediction is made by adding the predicted interannual increment in the target forecast year to the observation in the previous year.

2.3.2 Evaluation metrics

In this study, the anomaly correlation coefficient (ACC), the temporal correlation coefficients (TCC), and the precipitation anomaly percentage (PAP; Eq. 1) of summer precipitation were calculated to evaluate the prediction skill of the downscaling methods.

$$\mathrm{PAP} = \frac{P - \bar{P}}{P} \times 100\% \tag{1}$$

where P represents the precipitation of a certain period and $\bar{P}$ represents multi-year averaged precipitation.

In addition, the China Meteorological Administration's climate business prediction scoring (PS) standard is used to assess the degree of proximity between the predicted anomaly percentage and the observed anomaly percentage. This metrics can standardize the quality assessment of climate prediction and encourage the prediction of anomaly levels (Liu et al. 2016). The PS score is defined according to a six-level grading system (Table 1). The maximum and minimum scores are 100 and 0, respectively. The score is 100 when the anomaly percentage of prediction is consistent with the actual observation in both the sign symbol and the order of magnitude. When the predicted magnitude differs from the observed magnitude by one order, PS score is reduced by 20 to 0. In addition, prediction of abnormal precipitation is encouraged in this standard. 10 points will be added to the above score if an abnormal precipitation is reasonably predicted while the prediction differs from the observation by an order of magnitude (see Table 2 for the definition of PS score for all the six-level grading standard).

3 Results

3.1 Original prediction by the BCC_CSM1.1(m)

Figure 2 shows the distributions of the observed and predicted summer precipitation in Chongqing during 1991–2013. The summer precipitation in Chongqing is affected by the southwestern monsoon and topography. The distribution of summer precipitation is inhomogeneous in this region (Fig. 2a). The precipitation is lowest in the central region (Fengdu,

Table 1 The China Meteorological Administration's climate business prediction scoring (PS) standard according to a six-level grading system

Term	Especially less	Less	Slightly less	Slightly more	More	Especially more
ΔR	$\Delta R \le -50\%$	$-50\% < \Delta R \le -20\%$	$-20\% < \Delta R < 0$	$0 \le \Delta R < 20\%$	$20\% \le \Delta R < 50\%$	$50\% \le \Delta R$

Table 2 Six-grading systems for precipitation trend prediction

Observed trend level	Predicted trend level					
	Especially less	Less	Slightly less	Slightly more	More	Especially more
Especially less	100	80 + 10	60	20	0	0
Less	80 + 10	100	80	40	20	0
Slightly less	60	80 + 10	100	60	40	20
Slightly more	20	40	60	100	80 + 10	60
More	0	20	40	80	100	80 + 10
Especially more	0	0	20	60	80 + 10	100

4.2 mm day^{-1}) and increases towards the northeastern and southeastern. The extreme-low precipitation is found in western Chongqing, with average value ranging from 4.8 to 5.7 mm day^{-1}. The precipitation magnitude in southeastern and northeastern Chongqing is relatively larger, with average of greater than 5.7 mm day^{-1} (Xiushan, 6.3 mm day^{-1}; Youyang, 6.2 mm day^{-1}).

Generally, the distributions of the summer precipitation prediction are different from the actual observations. For all the model predictions at different lead times, more precipitation is found in northeastern and southeastern regions but less precipitation is found in central and western regions of Chongqing, with ACC values ranging from 0.37 to 0.42 (Fig. 2b–e). The BCC_CSM1.1(m) obviously underestimated summer precipitation by 2.1–2.9, 1.9–2.4, 1.8–2.6, and 1.6–2.4 mm day^{-1} in southeastern, western, northeastern, and central parts of Chongqing, respectively. Although the spatial heterogeneity of precipitation is basically captured, the high-value centers (Chengkou station in the northeast, Xiushan station in the southeast) and small-value centers (Fengdu station in the central) of precipitation are not found in these figures. This is mainly because the BCC_CSM1.1(m) underestimates the water vapor transported from northeastern Bay of Bengal, resulting in less summer precipitation in the central and eastern China (Wang et al. 2016).

Figure 3 shows the distributions of the correlation coefficients between the summer precipitation observation and predictions of different lead times during 1991–2013. The precipitation is underestimated by the LM0, LM1, LM2, and LM3 predictions, but similar distributions are obtained for the interannual increment of summer precipitation in various predictions (Figs. 2 and 3). Therefore, the error in the original prediction of the BCC_CSM1.1(m) does not change obviously with lead time. Possibly, the prediction skill of the summer precipitation in Chongqing in the model could only be improved by modifying the dynamical and physical processes in the model, for example, optimizing the boundary forcing field, the physical process, and the internal dynamics of the atmosphere, and improving the resolution of the model (Wang et al. 2008). Currently, the optimization of climate models is an important way to improve the prediction accuracy in provincial or national climate prediction services.

3.2 The optimal predictors for summer precipitation prediction

Figure 4 shows the optimal windows of the H_{500}, SST, U_{850}, and V_{850} in LM0 for the 34 stations in Chongqing. Among the H_{500} optimal windows, 71.4% of the windows are located in the mid-high latitudes and 23.6% are located from the eastern coast of China to the western Pacific. Li et al. (2011) also reported the good relationship between summer precipitation in Chongqing and the H_{500} in remote areas, for example, the blocking high in the mid-high latitudes (Ural Mountains, Lake Baikal, Sea of Okhotsk), the east Asia trough in mid-high latitudes (east Asia coast to west of Japan island), and the western Pacific subtropical high in summer. For the SST optimal windows, 35.3% were distributed in the western Pacific warm pool, and in the equatorial middle-eastern Pacific, 14.7% were distributed in the Indian Ocean, 11.7% were distributed in the Bay of Bengal, and 8.8% were distributed in the sea waters adjacent to China. Changes in SST in these areas affect the southwestern monsoon, the East Asian monsoon, and the western Pacific subtropical high, and thus result in changes of the rain belts in China (Liu et al. 2017; Lu et al. 2020; Wang and Chen 2018; Zhu et al. 2014 2020). Han et al. (2017) found that the higher SST in the eastern equatorial Pacific in summer would result in the stronger subtropical high in the Western Pacific, the weaker East Asian summer monsoon, and the more rainfall in the Yangtze River Basin. For the U_{850} optimal windows, 47.1% are distributed from the Iran plateau to Taiwan of China, and 23.5% are distributed from the Philippines to South China. For the V_{850} optimal windows, 38.2% are distributed from the Ural Mountains to Lake Baikal, 14.7% are distributed in the Bay of Bengal, and 20.6% are distributed near the Philippines and the South China Sea. Liu et al. (2015) pointed out that the South China Sea and the Bay of Bengal are the main sources of water vapor in East Asia, and the 850-hPa meridional winds transport water vapor from sea to land. Therefore, the spatial distributions of the above four predictors are scattered, but there are still some rules to follow. The

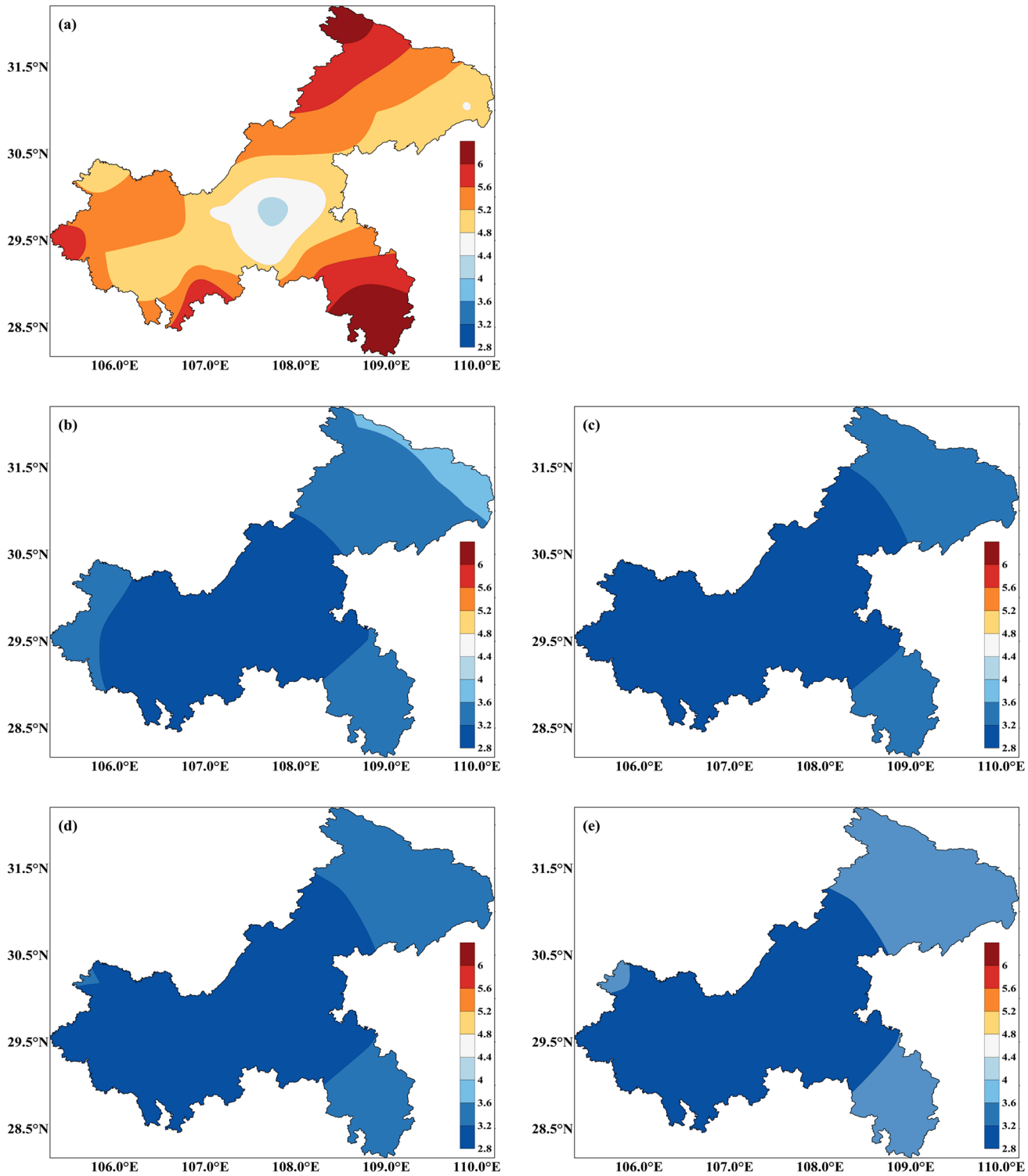

Fig. 2 Daily mean values of the observed (**a**) and BCC_CSM1.1(m) predicted (**b**–**e**) summer precipitation (unit: mm d^{-1}) in Chongqing during 1991–2013. Shown are the results for predictions at lead time of 0 month (LM0; **b**), 1 month (LM1; **c**), 2 months (LM2; **d**), and 3 months (LM3; **f**), respectively

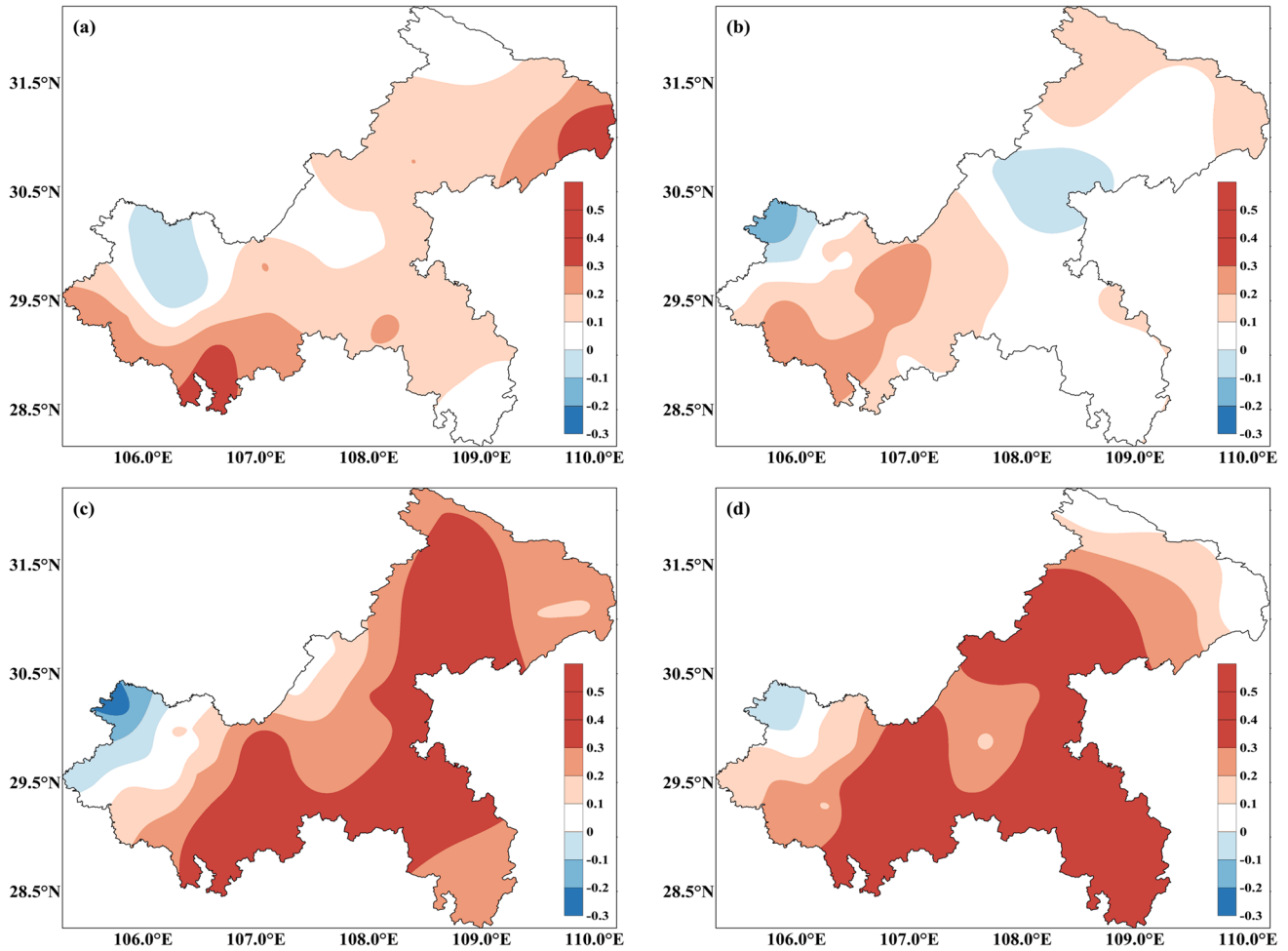

Fig. 3 Anomaly correlation coefficients between the observed and predicted interannual increments of summer precipitation in Chongqing during 1991–2013. The lead times of predictions are 0 month (LM0; **a**), 1 month (LM1; **b**), 2 months (LM2; **c**), and 3 months (LM3; **d**), respectively

predictors may have physical connections with precipitation at specific stations. For example, the atmospheric circulation in the mid-high latitudes and subtropical regions, the SST anomalies in offshore waters of China, and the western Pacific warm pool have obvious influences on the summer precipitation in Chongqing.

3.3 *LOO-CV for* in situ *precipitation prediction during 1991–2013*

Taking the LM0 prediction as an example, the 10-year running average TCCs between the interannual increment of each predictor and the observed summer precipitation at Shapingba, Wanzhou, and Qianjiang stations in 1991–2013 are examined (Fig. 5). The TCCs over these three stations fluctuate around 0.47, 0.58, − 0.71, and 0.39 for Shapingba (Fig. 5a), 0.78, 0.72, 0.70, and − 0.64 for Wanzhou (Fig. 5b), and 0.69, 0.75, 0.76, and 0.81 for Qianjiang (Fig. 5c), respectively.

Figure 6 shows the observed and predicted interannual increments of summer precipitation at three stations in Chongqing. The fitting rates of the single-factor regression, the stepwise regression, and the multiple linear regression prediction approaches at Shapingba are 0.68, 0.79, 0.72, 0.76, 0.85, and 0.82, respectively. The predictions at each station could reasonably capture the changes in the interannual increment of precipitation with a quasi-two-year oscillation (positive abnormal interannual increment in the current year and negative abnormal interannual increment in the following year). In addition, trends in the predicted interannual increments in most years were consistent with the observations. The average consistency rates of different prediction approaches are 78.0%, 78.8%, and 81.5% for Shapingba, Wanzhou, and Qianjiang in 1991–2013, respectively. Compared with other prediction approaches, the stepwise

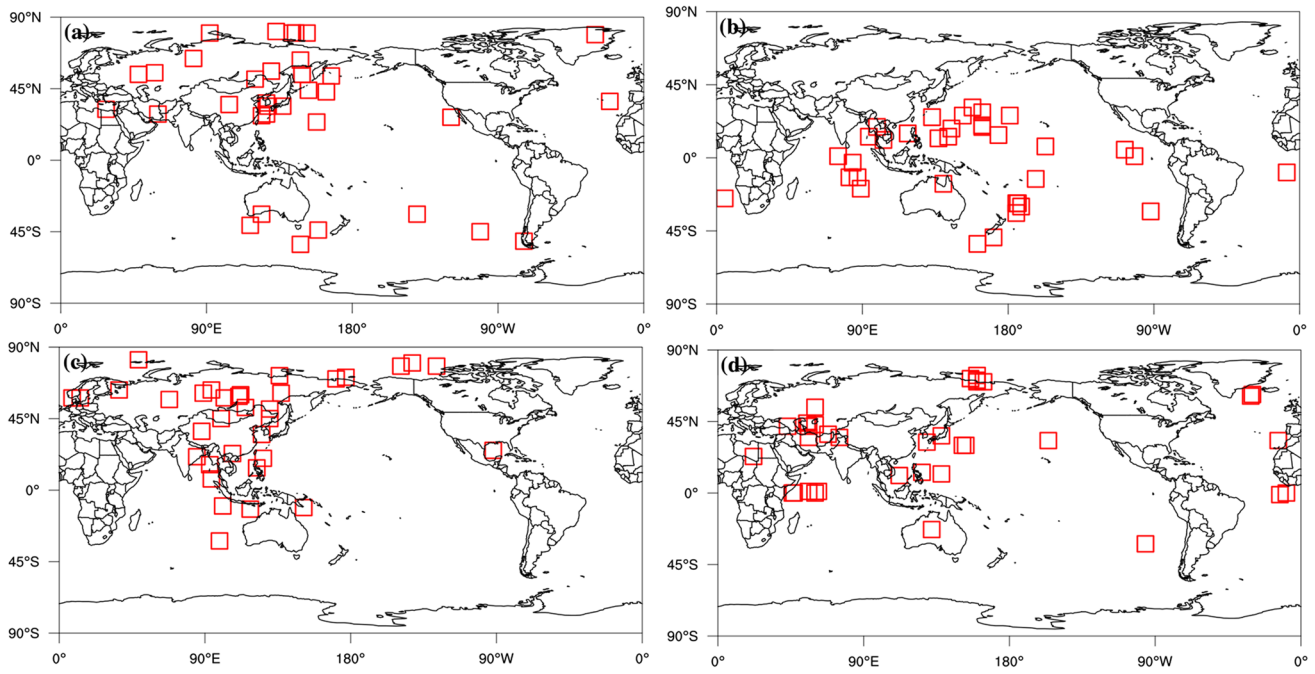

Fig. 4 Distribution of the optimal windows (red squares) with the highest correlation coefficients between interannual increment of summer precipitation and that of the predictor (H_{500}, **a**; SST, **b**; V_{850}, **c**; and U_{850}, **d**) at LM0 for the 34 weather stations in Chongqing

regression achieves the highest prediction accuracy, with a consistency rate of about 97%.

The performances of the downscaling methods in predicting the extreme wet case (i.e., 1998) and dry case (i.e., 2006) are shown in Table 3. In general, the original prediction skill of the wet case is much better than that of the dry case since the PS score is greater than 95 for all the predictions at different lead times in 1998. Considerable differences of PS are found in 2006, with 90.3 at LM3 but 0 at both LM0 and LM2. However, the poor prediction skill in 2006 could be obviously improved by using the downscaling method. Especially, the PS at LM0 and LM2 are improved by more than 60. For both the wet case and dry case, the prediction by the multi-factor regression approach is superior to the single-factor regression approach.

3.4 Prediction skill of summer precipitation during 2014–2018

Based on the optimal predictors of H_{500}, SST, U_{850}, and V_{850} corresponding to each station in Chongqing in 1991–2013, the regression function analysis is used to build downscaling methods for predicting the interannual increment of summer precipitation. Taking the Shapingba station as an example, the single-factor regression functions (Eqs. 2–5), the stepwise regression function (Eq. 6), and the multivariate regression function (Eq. 7) are established (Eqs. 2–7):

$$\mathrm{PI}_{\mathrm{H500}} = 0.08X_1 + 0.01 \tag{2}$$

$$\mathrm{PI}_{\mathrm{SST}} = 6.41X_2 + 0.01 \tag{3}$$

$$\mathrm{PI}_{\mathrm{U850}} = 1.04X_3 - 0.05 \tag{4}$$

$$\mathrm{PI}_{\mathrm{V850}} = -2.76X_4 - 0.01 \tag{5}$$

$$\mathrm{PI}_{\mathrm{S-Reg}} = 0.02X_1 + 3.56X_2 + 0.38X_3 - 1.01X_4 - 0.1 \tag{6}$$

$$\mathrm{PI}_{\mathrm{M-Reg}} = 0.01X_1 + 3.51X_2 + 0.31X_3 - 0.86X_4 - 0.09 \tag{7}$$

where PI is the predicted interannual increment of precipitation. X_1, X_2, X_3, and X_4 are the optimal predictors of H_{500}, SST, U_{850}, and V_{850}, respectively. S-Reg is the stepwise multiple regression, and M-Reg is the multiple regression. By comparing the regression coefficient of each predictor, it is found that the contributions of H_{500}, U_{850}, and V_{850} are similar, while SST has an especially prominent influence.

Table 4 shows the PS score of the BCC_CSM1.1(m), the single-factor linear regression, the stepwise regression, and the multivariate regression approaches for precipitation prediction during 2014–2018. Compared with the original prediction, all of the downscaling methods improve the prediction skills. The averaged PS scores increase to 81.7, 83.9, 80.1, 81.8, 85.4, and 85.3 in the five years, respectively.

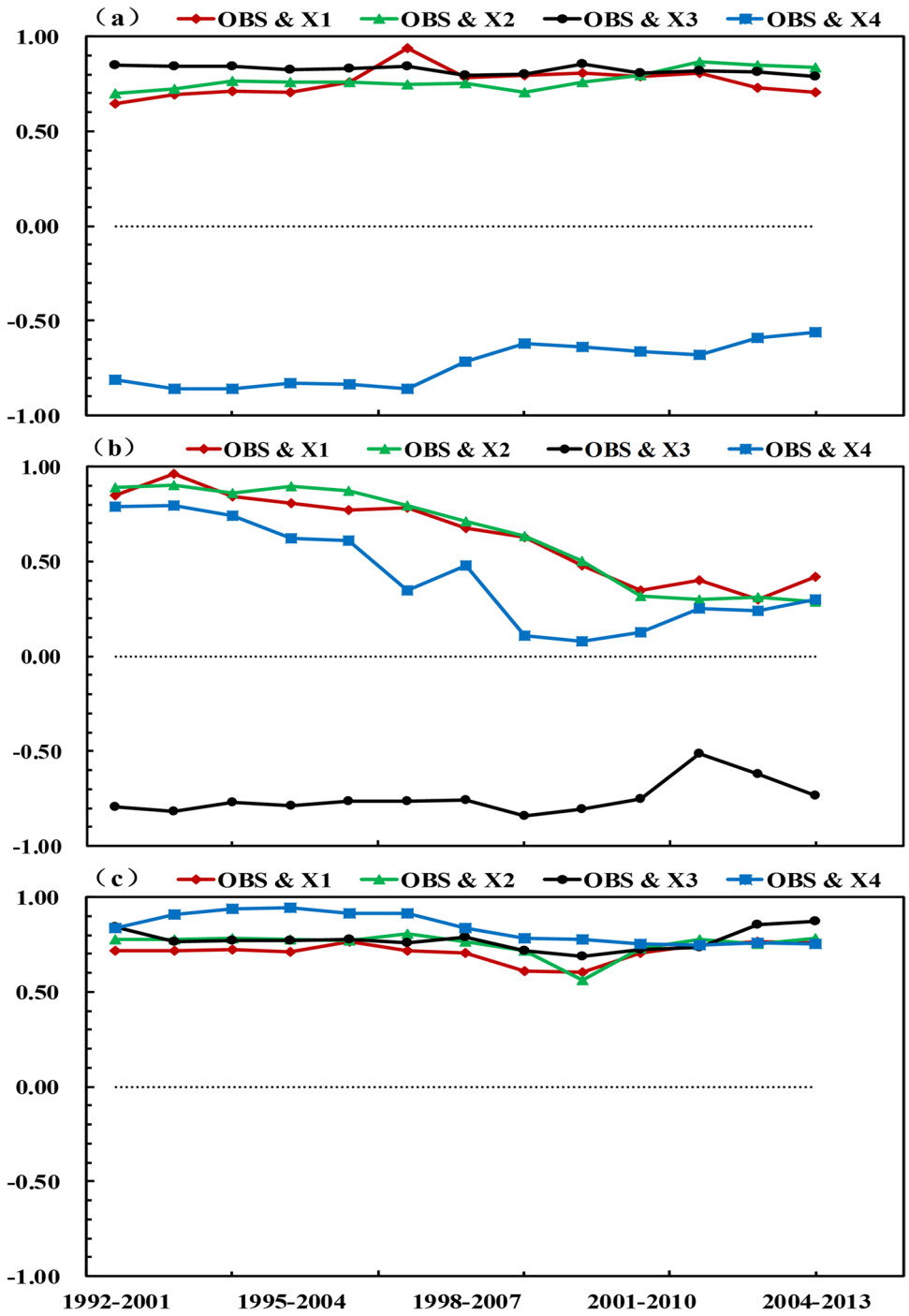

Fig. 5 The 10-year moving averaged temporal correlation coefficients (TCCs) between the interannual increment of the observed precipitation and the interannual increment of the four optimal predictors at LM0 during 1991–2013. The results are for the predictions of precipitation at Shapingba (**a**), Wanzhou (**b**), and Qianjiang (**c**). OBS, X_1, X_2, X_3, and X_4 represent interannual increment of observed precipitation, H_{500}, SST, V_{850}, and U_{850}, respectively

Especially, the improvements of prediction skill are more significant when the original predictions of the BCC_CSM1.1(m) are poor in several cases.

Figures 7 and 8 show the distributions of anomaly percentage of summer precipitation for the observations, the original predictions, and the corrected predictions with downscaling methods in 2017 and 2018, respectively. In 2017, the observed precipitation is relatively high in northeastern Chongqing but low in the rest areas (Fig. 7a). Compared with the observations, the model prediction at LM0 is basically similar in northeastern Chongqing, but obviously different in the rest areas. The PS of the original prediction averaged over the whole Chongqing is only 43. The single-factor stepwise regression and the multivariate regression approaches with the optimal predictors of H_{500}, SST, V_{850}, and U_{850} can clearly reduce the prediction errors of regional summer precipitation (Fig. 7c, d, e, and f). The spatial areas and amplitudes of abnormally low precipitation

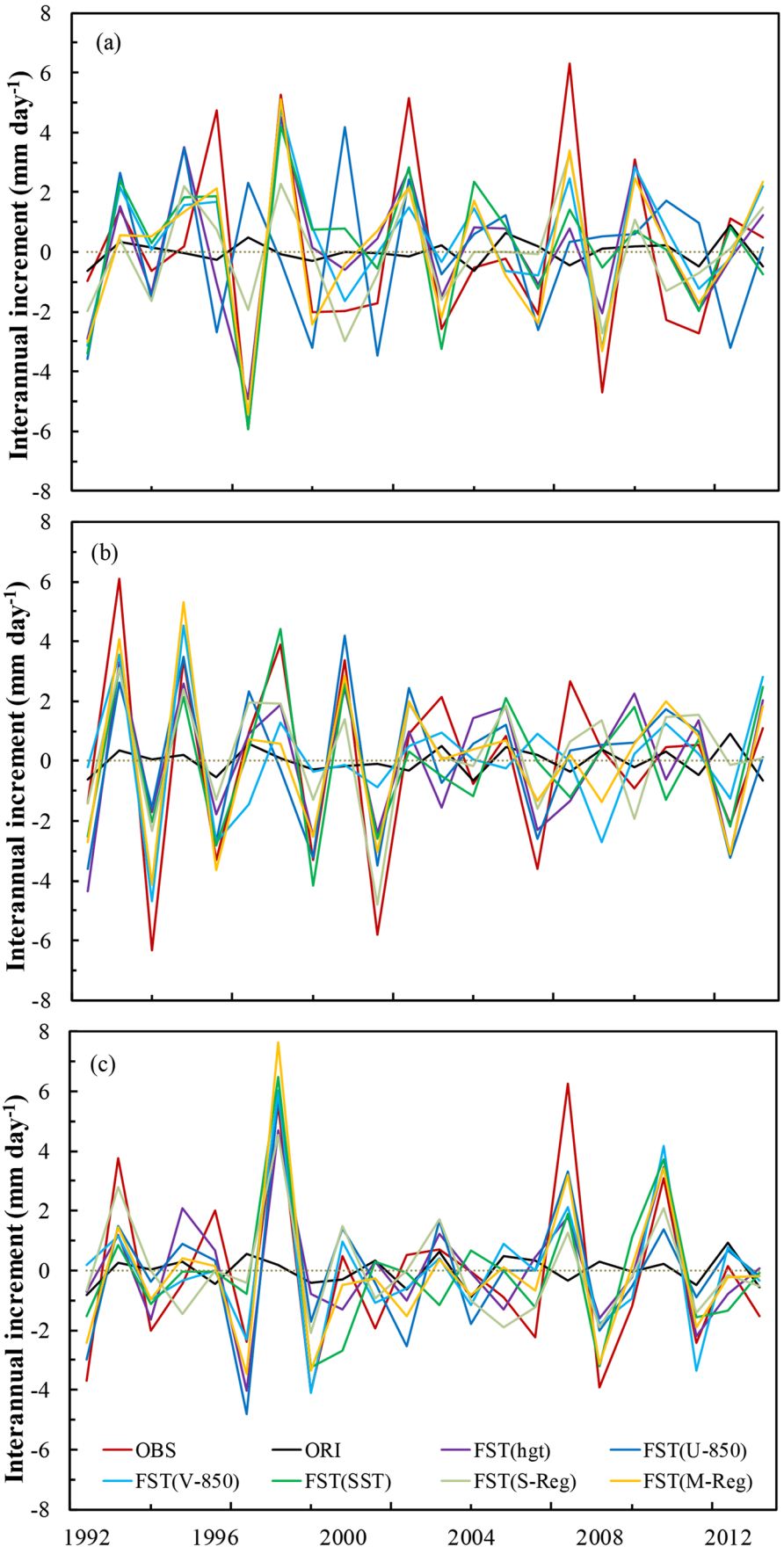

Fig. 6 Observed and predicted interannual increments of summer precipitation at LM0 with the leave-one-out cross-validation (LOO-CV) method during 1991–2013. The results are for the predictions of precipitation at Shapingba (**a**), Wanzhou (**b**), and Qianjiang (**c**). OBS, ORI, S-Reg, and M-Reg represent observation, model original prediction, stepwise regression prediction, and multivariate regression prediction, respectively

Table 3 PS scores of original forecast and single-factor linear regression, stepwise regression, and multivariate regression approaches forecast based on H_{500}, SST, V_{850}, and U_{850} in 1998 and 2006

Leading time	Year	Original prediction	Single-factor regression				Multi-factor approaches	
			H_{500}	SST	V_{850}	U_{850}	Stepwise	Multivariate
LM0	1998	95.7	92.1	96.3	94.8	95.9	96.5	96.5
	2006	0.0	62.7	72.4	62.5	69.8	73.5	68.9
LM1	1998	94.1	94.7	96.3	92.2	95.5	95.1	96.3
	2006	58.3	69.8	64.1	65.5	74.8	76.9	81.8
LM2	1998	96.2	93.1	95.7	85.2	89.9	96.3	96.2
	2006	0.0	67.5	62.5	78.7	81.4	74.8	71.1
LM3	1998	97.1	91.1	97.1	95.5	96.8	97.7	96.9
	2006	90.3	80.2	93.2	87.9	90.2	94.5	96.0

Table 4 PS scores of summer precipitation predictions by the BCC_CSM1.1(m), the single-factor linear regression, the stepwise regression, and the multivariate regression approaches at different lead times during 2014–2018

Leading time	Year	Original prediction	Single-factor regression				Multi-factor approaches	
			H_{500}	SST	V_{850}	U_{850}	Stepwise	Multivariate
LM0	2014	76.4	77.3	78.6	81.4	72.7	81.0	76.4
	2015	87.3	88.6	90.7	89.5	89.2	89.2	94.9
	2016	83.6	84.2	83.1	83.6	82.4	84.8	85.7
	2017	43.0	78.9	85.3	84.8	92.9	86.6	84.6
	2018	85.8	90.1	86.8	90.5	88.3	93.2	87.5
LM1	2014	81.2	69.1	83.3	75.4	66.7	89.1	84.4
	2015	87.3	88.5	88.9	88.0	88.3	88.9	90.7
	2016	84.5	80.9	81.3	83.6	80.0	84.8	83.1
	2017	82.8	86.0	64.2	62.7	82.5	86.2	85.3
	2018	55.3	71.5	90.4	87.0	78.0	78.1	90.4
LM2	2014	78.7	82.5	78.7	73.3	67.9	80.6	78.0
	2015	87.3	90.7	90.7	88.9	88.0	91.9	92.1
	2016	84.5	87.6	84.8	86.5	85.3	85.3	88.9
	2017	41.9	62.0	81.8	77.4	65.5	76.7	70.0
	2018	82.8	82.9	86.5	74.6	85.7	83.7	83.4
LM3	2014	79.4	80.1	69.1	72.4	75.0	81.1	82.5
	2015	87.3	87.7	91.4	87.3	88.6	88.5	89.2
	2016	83.6	80.2	84.1	84.1	87.3	85.3	85.3
	2017	80.7	80.7	85.3	57.1	79.2	82.5	86.6
	2018	89.8	84.6	94.3	74.4	91.9	91.4	88.6
Average		78.2	81.7	83.9	80.1	81.8	85.4	85.3

are also close to the observed distribution. The PS scores of the four single-factor linear regression with predictors of H_{500}, SST, V_{850}, and U_{850} are 78.9, 85.3, 84.8, and 92.9, respectively. The multi-factor predictor methods obviously improve the prediction skills of summer precipitation, with PS scores of 86.6 and 94.6 for the stepwise and multivariate regression approaches, respectively. Particularly, the multivariate regression approaches can reproduce the distribution of sporadic precipitation in the northeastern and southwestern Chongqing.

In 2018, there is more precipitation in Wulong (southeastern Chongqing), Jiangjin, Qijiang (southwestern Chongqing), and Tongnan (western Chongqing), but less rainfall in the rest regions (Fig. 8a). The original prediction at LM0 could generally reproduce precipitation distribution in most areas. However, area ranges with extreme-lower precipitation are much smaller than the actual observation (Fig. 8b). The single-factor linear regression, the stepwise regression, and the multiple regression approaches based on the predictors of H500 (Fig. 8c), SST (Fig. 8d), V850 (Fig. 8e), and U850 (Fig. 8f) further improve the prediction skills of summer precipitation. The distribution and decline of abnormal precipitation predicted by these regression methods are similar to the observations, with PS of 90.1, 86.8, 90.5, 88.3, 93.2, and 87.5, respectively. Among the above methods, the prediction method established with the multifactor stepwise regression approach shows the best prediction skill (Fig. 8g), especially at stations with precipitation

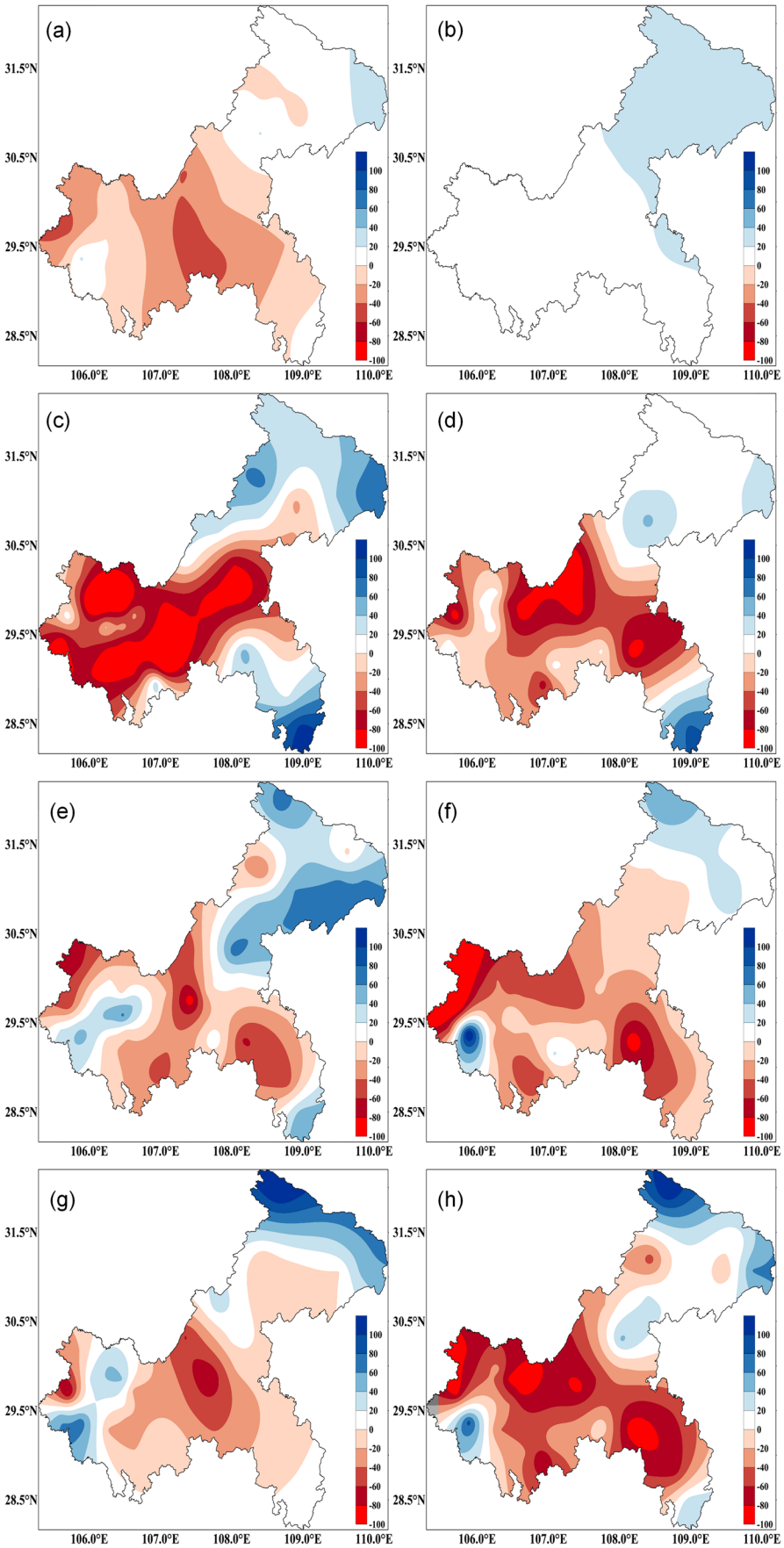

Fig. 7 Distribution of summer precipitation anomaly percentage in Chongqing in 2017. (**a**) Observation; (**b**) original prediction at LM0; (**c**–**f**) predictions with the single-factor linear regression approaches (H_{500}, SST, V_{850}, and U_{850}); (**g**) predictions with the stepwise multiple regression approaches; (h) predictions with the multivariate regression approaches

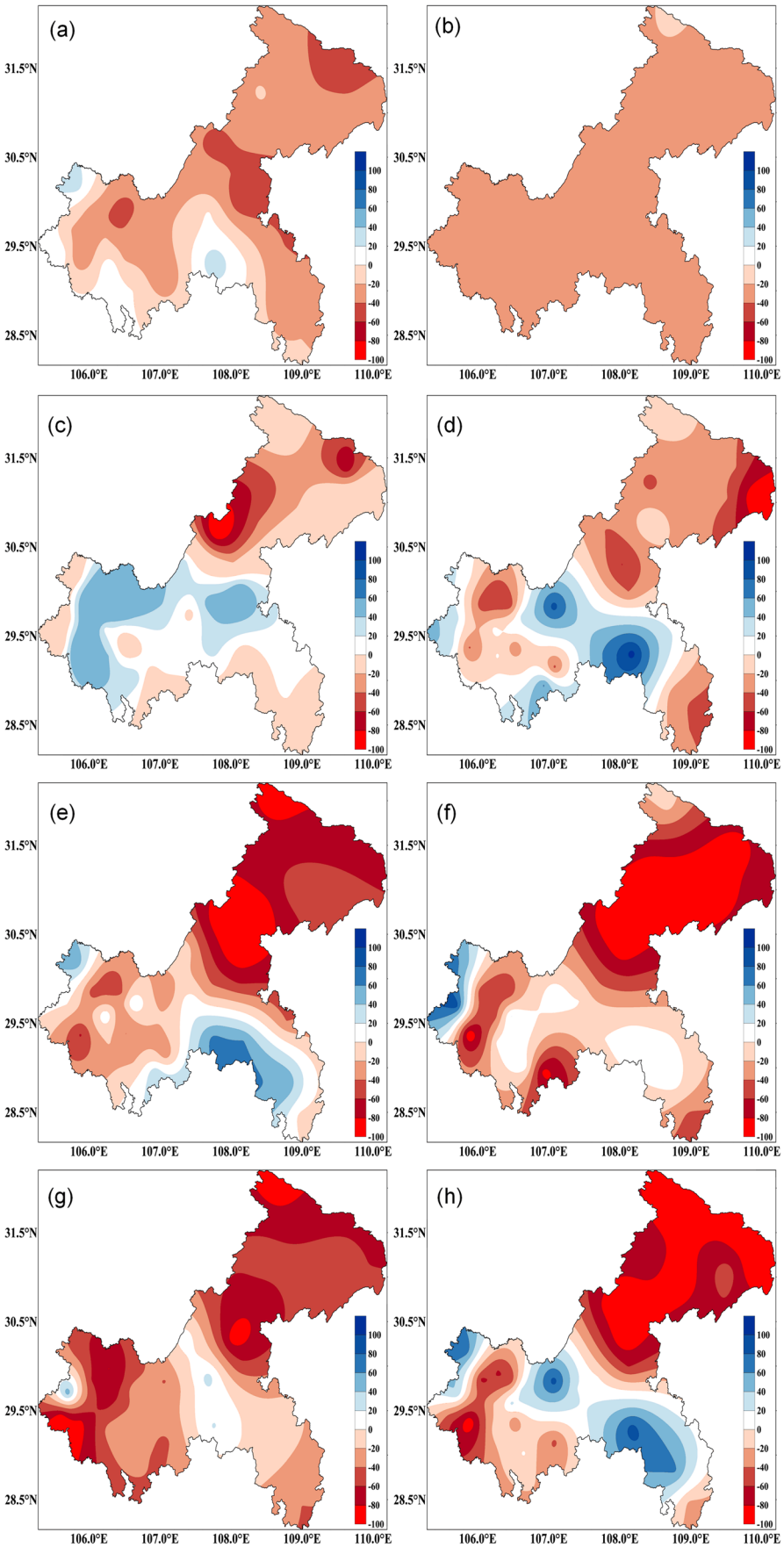

Fig. 8 Same as Fig. 7, but for prediction of precipitation in 2018

anomaly percentage increased by more than 50% (Wulong and Fengdu) or decreased by more than 50% (Qianjiang, Shizhu, Zhongxian, Liangping, Wuxi, and Beibei).

It is noted that the downscaling methods may obtain unsatisfactory predictions in several years, for example, the LM1 prediction by single-factor regression approach with H500 in 2016, with SST in 2017, with U850 in 2014, and with V850 in 2017; the LM3 prediction by single-factor regression approach with V850 in 2017; and the LM1 prediction by multivariate regression approach in 2016. The PS scores in the above cases are lower than those in the original predictions by the BCC_CSM1.1(m), indicating the uncertainty of statistics-based downscaling methods. Kug et al. (2008) and Wang et al. (2017) reported that more than 30-year observations were required to establish the prediction methods with stable precipitation prediction skills. Thus, the prediction skills shown in this study may be improved when more forecast data is used to establish the prediction method in future.

4 Conclusion

Based on the hindcast experiments of the BCC_CSM1.1(m) during 1991–2018, this study evaluates the ability of the model in predicting in situ summer precipitation in Chongqing in Southwest China. Besides, a downscaling method based on combination of the multiple regression approach, the interannual increment prediction approach, and the optimal window approach is used to correct summer precipitation prediction. The main conclusions are as follows:

1. The original predictions by the BCC_CSM1.1(m) capture the distribution feature of more precipitation in northeast and southeast, and less precipitation in western Chongqing. However, the model obviously underestimates summer precipitation and cannot reproduce the decreasing trend of summer precipitation in central Chongqing.
2. The downscaling method could obviously improve the prediction skills of summer precipitation in southwest China. Particularly, the downscaling method based on multi-factor stepwise regression approach has the highest prediction skill across years and sites. In addition, both the downscaling method and the BCC_CSM1.1(m) obtain good skills for the prediction of wet case but the former achieves apparently higher skills than the latter for the prediction of dry case.
3. The downscaling prediction method based on multivariate regression approach skillfully predicts the abnormal precipitation in 2017 and 2018, with similar magnitude of the anomalies as the actual precipitation. Overall, the downscaling method developed in this study can improve the prediction skill of in situ summer precipitation in Southwest China.

Generally, the downscaling prediction method established with the multi-factor stepwise regression approach obtains more stable and reasonable prediction skills in most years. The finding is worth for provincial or regional climate predictions. Next, we will take into account the physical mechanism and predictability of summer precipitation in the transition zone from the Qinghai-Tibet Plateau to the middle reaches of the Yangtze River in China, and explore the physical processes between large-scale circulation variables and summer precipitation in Chongqing. In addition, we will also consider using the slowly changing physical background information to correct the predictions.

Acknowledgements We thank the Climate Simulation Laboratory of National Climate Center which provided the simulation data of the BCC_CSM1.1(m) model.

Author contribution Qu Guo and Xiangwen Liu conceived the topic of the work. Hongyu Tang and Yonghua Li archived the datasets and drew the figures. Qu Guo drafted the manuscript, and Xiangwen Liu revised the manuscript. All the authors of this article reach a consensus on the participation in and publication of this article.

Funding This study was supported by the National Natural Science Foundation of China (41875111, 41605068) and the Forecasters' Project of China Meteorological Administration (CMAYBY2019-096).

Data availability • The data, materials and codes of this article can be obtained by contacting the corresponding authors at guoqu510@163.com and xwliu@cma.gov.cn.

None of the authors' research deals with ethical issues.

Declarations

Conflict of interest The authors declare no competing interests.

References

Bollasina MA, Ming Y (2013) The general circulation model precipitation bias over the southwestern equatorial Indian Ocean and its implications for simulating the South Asian monsoon. Climate Dyn 40:823–838. https://doi.org/10.1007/s00382-012-1347-7

Fan K, Wang HJ (2009) A new approach to forecasting typhoon frequency over the western North Pacific. Wea Forecasting 24:974–978. https://doi.org/10.1175/2009WAF2222194.1

Fan K, Lin MJ, Gao YZ (2009) Forecasting the summer rainfall in North China using the year-to-year increment approach. Sci China Ser d: Earth Sci 52:532–539. https://doi.org/10.1007/s11430-009-0040-0

Fan K, Liu Y, Chen H (2012) Improving the prediction of the East Asian summer monsoon: new approaches. Weather Forecast 27:1017–1030. https://doi.org/10.1175/WAF-D-11-00092.1

Fan K, Wang H, Choi YJ (2008) A physically-based statistical forecast model for the middle-lower reaches of the Yangtze River Valley

summer rainfall. Chin Sci Bull 53:602–609. https://doi.org/10.1007/s11434-008-0083-1
Gong Z, Dogar MM, Qiao S et al (2018) Assessment and correction of BCC_CSM's performance in capturing leading modes of summer precipitation over North Asia. Int J Climatol 38:2201–2214. https://doi.org/10.1002/joc5327
Gu WZ, Chen LJ, Li WJ et al (2011) Development of a downscaling method in China regional summer precipitation prediction. J Meteor Res 25:303–315. https://doi.org/10.1007/s13351-011-0306-2
Han TT, He SP, Wang HJ et al (2017) Enhanced influence of early-spring tropical Indian Ocean SST on the following early-summer precipitation over Northeast China. Climate Dyn 51:4065–4076. https://doi.org/10.1007/s00382-017-3669-y
Hu YR, Maskey S, Uhlenbrook S (2013) Downscaling daily precipitation over the Yellow River source region in China: a comparison of three statistical downscaling methods. Theor Appl Climatol 112:447–460. https://doi.org/10.1007/s00704-012-0745-4
Ji JJ, Huang M, Li KR (2008) Prediction of carbon exchanges between China terrestrial ecosystem and atmosphere in the 21st century. Sci China: Earth Sci 51:885–898. https://doi.org/10.1007/s11430-008-0039-y
Jiang DB, Tian Z, Lang X (2016) Reliability of climate models for China through the IPCC Third to Fifth Assessment Reports. Int J Climatol 36:1114–1133. https://doi.org/10.1002/joc4406
Juneng L, Tangang FT, Kang H et al (2010) Statistical downscaling forecasts for winter monsoon precipitation in Malaysia using multimodel output variables. J Climate 23:17–27. https://doi.org/10.1175/2009JCLI28731
Kan M, Huang A, Zhao Y et al (2015) Evaluation of the summer precipitation over China simulated by BCC_CSM model with different horizontal resolutions during the recent half century. J Geophys Res Atmos 120:4657–4670. https://doi.org/10.1002/2015JD023131
Kang HW, Park C, Hameed S et al (2009) Statistical downscaling of precipitation in Korea using multimodel output variables as predictors. Mon Wea Rev 137:1928–1938. https://doi.org/10.1175/2008MWR27061
Kang HW, Zhu CW, Zuo ZY (2011) Statistical downscaling of pattern projection using multi-model output variables as predictors. J Meteor Res 25:293–302. https://doi.org/10.1007/s13351-011-0305-3
Kohavi R (1995) A study of cross-validation and bootstrap for estimation and model selection. Proc. of the 14th Int. Joint Conf. on Artificial Intelligence, Morgan Kaufmann Publishers, 1137–1143.
Kug J, Lee J, Kang I (2008) Systematic error correction of dynamical seasonal prediction of sea surface temperature using a stepwise pattern project method. Mon Wea Rev 136:3501–3512. https://doi.org/10.1175/2008MWR22721
Li J, Wang B (2018) Origins of the decadal predictability of East Asian land summer monsoon rainfall. J Clim 31:6229–6243. https://doi.org/10.1175/JCLI-D-17-0790.1
Li YH, Xu HM, Liu D (2011) Features of the extremely severe drought in the east of southwest China and anomalies of atmospheric circulation in summer 2006. J Meteor Res 25:176–187. https://doi.org/10.1007/s13351-011-0025-8
Liu Y, Fan K (2014) An application of hybrid downscaling model to forecast summer precipitation at stations in China. Atmos Res 143:17–30. https://doi.org/10.1016/j.atmosres.2014.01.024
Liu JP, Li WJ, Chen LJ et al (2016) Estimation of the monthly precipitation predictability limit in China using the nonlinear local Lyapunov exponent. J Meteor Res 30:93–102. https://doi.org/10.1007/s13351-015-5049-z
Liu XW, Wu TW, Yang S et al (2014) Relationships between interannual and intraseasonal variations of the Asian-western Pacific summer monsoon hindcasted by BCC_CSM11 (m). Adv Atmos Sci 31:1051–1064. https://doi.org/10.1007/s00376-014-3192-6
Liu XW, Wu TW, Yang S (2015) Performance of the seasonal forecasting of the Asian summer monsoon by BCC_CSM1.1(m). Adv Atmos Sci 32:1156–1172. https://doi.org/10.1007/s00376-015-4194-8
Liu YJ, Ding YH, Zhang YX et al (2017) Role of a warm and wet transport conveyor of Asian summer monsoon in Beijing heavy rainstorm on July 21 2012. J Trop Meteorol 23:302–313
Lu R, Zhu Z, Li T et al (2020) Interannual and interdecadal variabilities of spring rainfall over northeast China and their associated sea surface temperature anomaly forcing. J Climate 33(1423–1435):52. https://doi.org/10.1175/JCLI-D-19-0302.1
Murray RJ (1996) Explicit generation of orthogonal grids for ocean models. J Comput Phys 126:251–273. https://doi.org/10.1006/jcph19960136
Paul S, Liu CM, Chen JM et al (2008) Development of a statistical downscaling model for projecting monthly rainfall over East Asia from a general circulation model output. J Geophys Res 113:D15117. https://doi.org/10.1029/2007JD009472
Wang L, Chen G (2018) Impact of the spring SST gradient between the tropical Indian Ocean and Western Pacific on landfalling tropical cyclone frequency in China. Adv Atmos Sci 35:682–688
Wang B, Li J, Cane M, Liu J et al (2018) Towards predicting changes in the land monsoon rainfall a decade in advance. J Clim 31:2699–2714. https://doi.org/10.1175/JCLI-D-17-0521.1
Wang L, Ren HL, Chen QL et al (2017) Statistical correction of ENSO prediction in BCC_CSM11m based on stepwise pattern projection method. Meteor Mon 43:294–304. https://doi.org/10.7519/jissn1000-0526201703005(inChinese)
Wang L, Ren HL, Zhu JS et al (2020) Improving prediction of two ENSO types using a multi-model ensemble based on stepwise pattern projection model. Climate Dyn 54:3229–3243. https://doi.org/10.1007/s00382-020-05160-2
Wang Q, Huang AN, Zhao Y et al (2016) Evaluation of the precipitation seasonal variation over eastern China simulated by BCC_CSM model with two horizontal resolutions. J Geophys Res Atmos 121:8374–8389. https://doi.org/10.1002/2016JD024959
Winton M (2000) A reformulated three-layer sea ice model. J Atmos Ocean Tech 17(4):525–531. https://doi.org/10.1175/1520-0426(2000)017%3c0525:ARTLSI%3e2.0.CO;2
Wu TW, Yu RC, Zhang F et al (2010) The Beijing Climate Center atmospheric general circulation model: description and its performance for the present-day climate. Climate Dyn 34:123–147. https://doi.org/10.1007/s00382-008-0487-2
Wu TW, Li WP, Ji JJ et al (2013) Global carbon budgets simulated by the Beijing Climate Center Climate System Model for the last century. J Geophys Res-Atmos 118(10):4326–4347. https://doi.org/10.1002/jgrd.50320
Zhu Z, Li T, He J (2014) Out-of-phase relationship between boreal spring and summer decadal rainfall changes in southern China. J Climate 27:1083–1099. https://doi.org/10.1175/JCLI-D-13-00180.1
Zhu Z, Lu R, Yan H et al (2020) The dynamic origin of the interannual variability of West China autumn rainfall. J Climate 33:9643–9652. https://doi.org/10.1175/JCLI-D-20-0097.1
Zhu CW, Park CK, Lee WS et al (2008) Statistical downscaling for multi-model ensemble prediction of summer monsoon rainfall in the Asia-Pacific region using geopotential height field. Adv Atmos Sci 25:867–884. https://doi.org/10.1007/s00376-008-0867-x